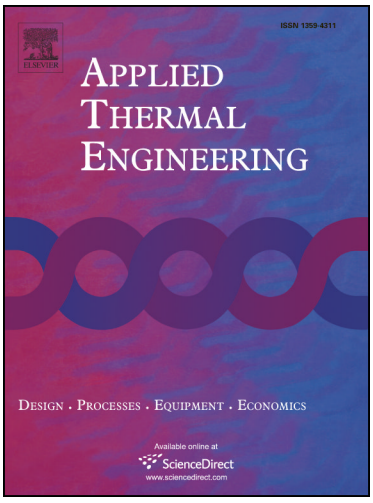

Development and Performance analysis of a TEG system using exhaust recovery for a light diesel vehicle with assessment of fuel economy and emissions

Eid S. Mohamed

PII: S1359-4311(18)30123-6
DOI: https://doi.org/10.1016/j.applthermaleng.2018.10.100
Reference: ATE 12844

To appear in: *Applied Thermal Engineering*

Received Date: 7 January 2018
Revised Date: 19 October 2018
Accepted Date: 22 October 2018

Please cite this article as: E.S. Mohamed, Development and Performance analysis of a TEG system using exhaust recovery for a light diesel vehicle with assessment of fuel economy and emissions, *Applied Thermal Engineering* (2018), doi: https://doi.org/10.1016/j.applthermaleng.2018.10.100

Development and Performance analysis of a TEG system using exhaust recovery for a light diesel vehicle with assessment of fuel economy and emissions

Eid S. Mohamed

Faculty of Engineering, Automotive and Tractors Engineering dep., Helwan University,
P.O. Box 11718, Mataria, Cairo, Egypt, Tel.: 00201006427775,
E-mail Address: Eng_eid74@yahoo.com.

Abstract

Exhaust heat from vehicle engines can be one of the promising heat sources to provide additional energy using thermoelectric generation (TEG). However, the objective of this study is to assess the exhaust heat recovery behavior by TEG, evaluation of diesel fuel consumption (DFC) and exhaust emissions. Thirty standard thermoelectric modules (TEMs) were mounted on the two sides (1x5) and lower side (4x5) arrangement of a light diesel vehicle exhaust channel. A detailed experimental work was carried out to study the performance behavior of TEG system with different engine speeds and over new European driving cycle (NEDC) using chassis dynamometer. Comparative analyses of the exhaust gases flow rate, DFC, exhaust emissions such as THC, CO, CO_2, and smoke emissions have been measured during NEDC with and without TEG actuation. Experimental results observed that the average value of TEG system efficiency is approximately 4.63% under the NEDC conditions. It also found that: by actuation the TEG system, the effectiveness of DFC percentage has been reduced by (1.46%-3.13%), lower exhaust gas emissions were found, too. The experimental result of output power is in good agreement with the theoretical result within 5.16% error at 1500 rpm.

Key words: Thermoelectric generator, diesel vehicles, fuel economy, exhaust gas emissions, waste heat recovery, NEDC.

1. Introduction

Around 35–40% of the fuel energy source to internal combustion engine (ICE) in vehicle is discharged as waste heat through the exhaust system **[1]**. The exhaust heat directly transformed into electricity by the thermoelectric generators (TEGs) has begun to enter automotive applications **[2, 3].** Over the last 20 years, there has been growing interest in applying of TEGs system to improve the efficiency of waste heat recovery, using the various heat sources such as geothermal energy **[4],** the applications of thermoelectricity have been

expanded from medical, military, and power plants **[5-8]** automotive **[9-14],** stove **[15-17]** and other industrial heat **[18–21].** The performance evaluations of series–parallel connection for TEMs by experiment and numerical solution are presented in **[22, 23].**

Eakburanawat and Boonyaroonate [24] described a thermoelectric battery charger powered by TEMs. A number of research groups have investigated the maximum power point tracking (MPPT) control method suitable for TEG systems **[25-27].** Most reported improvements of engine fuel consumption (EFC) by using the TEGs, in range 1-5% **[28-30]. Karri et al. [31]** created a comprehensive water-cooled TEG vehicle model including parasitic losses due to TEG weight and pressure drop, and a peak fuel efficiency increase of 1.25% was reported. **Nicholas, Yanliang [32]** presented the optimal design of TEG based on a light-duty passenger vehicle, and maximum fuel efficiency increase of 2.5% with TEMs. Some works use the new European driving cycle (NEDC) to evaluate engine operation **[33-35],** TE devices can also be used in conjunction with traditional CO_2 reduction approaches to further reduce greenhouse gas emissions **[36,37].**

The maximum output power of 944W for the TEG system application on automobiles was reported by **Liu et al. [38].** One useful application for the TEG device is as a source of electrical power generation in vehicles in allowance of or in addition to the alternator. Electrical loads in motor vehicles can be categorized as continuous electrical loads (ignition system, monitor screen, fuel system, etc.), long-time electrical loads (lighting, cassette car radio , etc.), short-time electrical loads (turn and stop lamps, cooling fan, electric windows, etc.) and seasonal loads (air conditioners and heaters). The alternator is the source of this power in addition to the power required to ensure adequate energy storage in the battery. The alternator is mechanically driven by the engine crank shaft and operates at an average efficiency of about 50%. **[39,40].**

Thus, the work presented here aims to develop a TEG system with a new procedure using thirty standard (TEG1B-12610-5.1) TEMs. The TEM type has been selected depending on maximum temperate on exhaust pipe. The TEG system was mounted to the exhaust pipe of a light diesel vehicle in order to supply heat. The airflow around TEG has been simulated in the cold side to reject heat. The TEG system performance is presented in details over the temperature range, different engine speeds and NEDC. The effects of TEG device on the vehicle engine performance including exhaust gases mass flow rate, DFC, exhaust emissions and smoke opacity emission have been analyzed during NEDC terms. A comparative analysis of the DFC and exhaust emissions such as THC, CO, CO_2, and smoke has been measured with and without actuation of the TEG device.

2. TEG model and thermal behavior

2.1 Theory and *Novel configuration of TEG*

The energy conversion process of a TEG is showed in **Fig. 1.** The thermoelectric module (TEM) is inserted between the hot source and the cold source. Thermal energy is converted into electrical energy due to the changes of internal quantum structure of the TE material. In order to realize the practical importance as a generator in heat recovery units, it is necessary to increase the conversion efficiency of the TE material and to improve the heat transfer from exhaust gas to the TEM, a thermoelectric module, p-type and n-type semiconductors are used instead of metal conductors **[41, 42].**

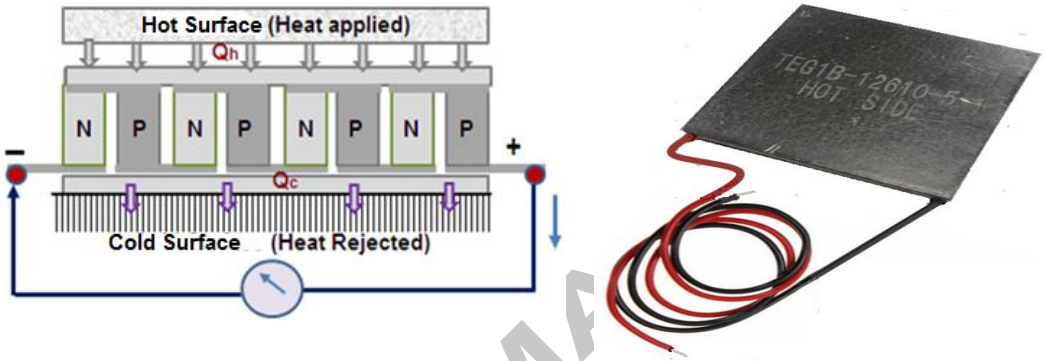

Fig. 1: Thermoelectric module

In this application the heat capacity of exhaust gas Q_{ex} is used in the following formula in order to estimate the heat energy as function of the temperatures:

$$Q_{ex} = \dot{m} C_p (T_{ex} - T_{\text{amb}}) \quad (1)$$

where T_{ex} is exhaust gas temperature, T_{amb} is ambient temperature, the exhaust gas flow rate ($\dot{m}$) is the sum of the air flow and the fuel flow through the cylinder or it is measured, C_p is the heat capacity of the exhaust gas. The efficiency of thermoelectric elements in converting heat to electricity can be calculated using

$$\eta_{th} = \left[\frac{T_h - T_c}{T_c}\right]\left[\frac{(1+ZT)^{0.5} - 1}{(1+ZT)^{0.5} + (T_c / T_h)}\right] \quad (2)$$

where ZT is the figure of merit, and T_h and T_C are the hot-side and cold-side temperatures of the thermoelectric materials, respectively. A figure of merit $Z = \alpha^2 \delta / K$, is used to define the performance of a thermoelectric material. It is derived from (α) the Seebeck coefficient, (δ) electrical conductivity, and (K) thermal conductivity of the material, and T is the average temperature between hot and cold surfaces of the TEG, $T = (T_c + T_h)/2$.

The increase in generated power and fuel economy enhancement takes place because the insulation has increased the heat input (Q_i), which expresses generated power, and the enhancement is conspicuous in the high-temperature type elements because the rate of increase in the heat input from before insulation to after insulation is greater in the high-temperature type elements than it is in the low-temperature type elements

$$P_o = V_o I_o = \eta_{th} Q_h = Q_h - Q_c \quad (3)$$

where P_o is the generated power, η_{th} efficiency of thermoelectric elements, Q_h heat input, Q_c heat removal, and the output current and voltage I_0 and V_o respectively.

The rate of heat supply at hot side of thermocouples

$$Q_h = \alpha I T_h + \frac{R_c I^2}{2} + K\Delta T \quad (4)$$

The rate of heat removal at cold side of TEG

$$Q_c = \alpha I T_c - \frac{R_c I^2}{2} + K\Delta T \quad (5)$$

where I is the generated current, R_C is the internal electrical resistance, the temperature difference across the couple $\Delta T = T_h - T_c$

According to Eqs. (4) and (5), inserting into Eq. (3),

$$P_o = \alpha I \Delta T + R_c I^2 \quad (6)$$

The current and voltage through the load are

$$I_o = \frac{\alpha \Delta T}{R_c + R_L} \qquad V_o = \frac{P_o}{I_o} = \alpha \Delta T - I R_C \quad (7)$$

For the Fourier effect, the rate of heat supplied Q_h by heat source and rate of heat removal Q_c by heat sink can be expressed as:

$$Q_h = K_h (T_h - T_1) \quad and \quad Q_c = K_c (T_2 - T_c) \quad (8)$$

where K_h and K_c are called the total hot-side thermal conductivity and K_c the total cold-side thermal conductivity respectively. R_L is the load resistance, T_1 is the temperature of hot side of thermocouples, and T_2 is the temperature of cold side of Thermocouples. The output power of the parallel TEG is given by,

$$P_o = I_o^2 R_L$$

2.2 TEMs system array design

One of the main considerations in the design of large TEG power system is to select suitable TE modules which meet the specific requirements of application and arrange them into an appropriate configuration to meet the specification. In order to provide the required power output, modules can readily be arranged in an array and connected electrically in series and/or parallel. The method of correlation of TEGs is usually estimated by the desired voltage and / or current **[42].**

The series array of TEG circuit can be seen approximately as a simple series circuit shown in **Fig. 2a,** each TEG within the array will experience an equal ΔT and therefore all TEGs will produce an equal output voltage V_0 and the array will be in a balanced thermal condition. According to Kirchhoff's law, in a series circuit the total voltage V_o is equal to the sum of the voltages in each individual TEG branch.

$$V_o = V_1 + V_2 + V_3 + \cdots V_N = \sum_{i=1}^{N} V_i \qquad and \qquad I_o = \frac{V_o - V_S}{\sum_{i=1}^{N} R_i} \tag{9}$$

The parallel TEG circuit can be seen approximately as a simple series circuit shown in **Fig. 2b.** According to Kirchhoff's law, I_o is equal the sum of the currents in each individual branch.

$$I_o = I_1 + I_2 + I_3 + \cdots I_N = \sum_{i=1}^{N} I_i \tag{10}$$

$$I_1 = \frac{V_1 - V_p}{R_1} \qquad I_2 = \frac{V_2 - V_p}{R_2} \qquad \therefore I_i = \frac{V_i - V_p}{R_i} \tag{11}$$

Where V_S and V_P are the voltage at the terminals for series and parallel array's, $V_L = V_o - I_o R_{\text{int}}$

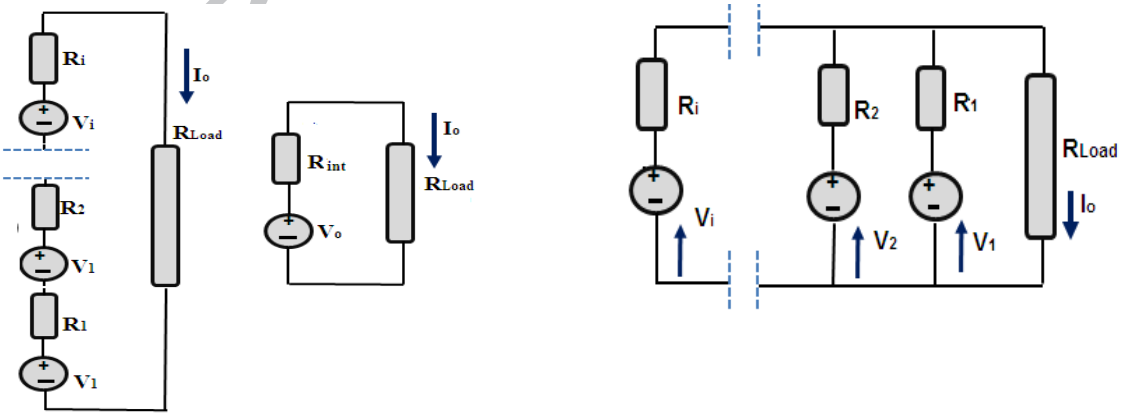

(a) Series connection

(b) Parallel connection

Fig. 2: Electrical diagram of an array of TEMs electrically connected in series and parallel.

2.3 power conditioning system

The TE power conditioner, which maintains the optimum electrical condition of the TEG modules, it consists of the three different subsystems, a DC–DC boost converter, the maximum power point tracking (MPPT) controller and the battery. The 30 TEMs in **Fig. 3a** are grouped into three units; the three units are connected in parallel arrays. A DC–DC converter mounted between TEMs and a load works as an impedance converter. The converter consists of an inductor, a switch; a capacitance and a diode, the electronic elements specification and connection are described in more detail in the literature **[25,43].**

The TE power conditioner with MPPT control is inserted between TEMs and the battery. The MPPT controller is digitally implemented by a simple microcontroller which possesses an analog-to-digital converter (ADC) to take the feedback signals and a direct pulse-width-modulated (PWM) output to converter drive MOSFET of the boost converter.

Fig. 3b shows the proposed MPPT circuit, the battery discharging mode is governed by the voltage control loop, while later three modes are governed by the MPPT control. In the large load mode, both the TEG and the battery supply power to the load. In the small load mode, the extra power is used to charge the battery to balance the output power of the TEG and needed power of the load. In the optimal load mode, the maximum power is drawn from the TEG and transferred to the load totally.

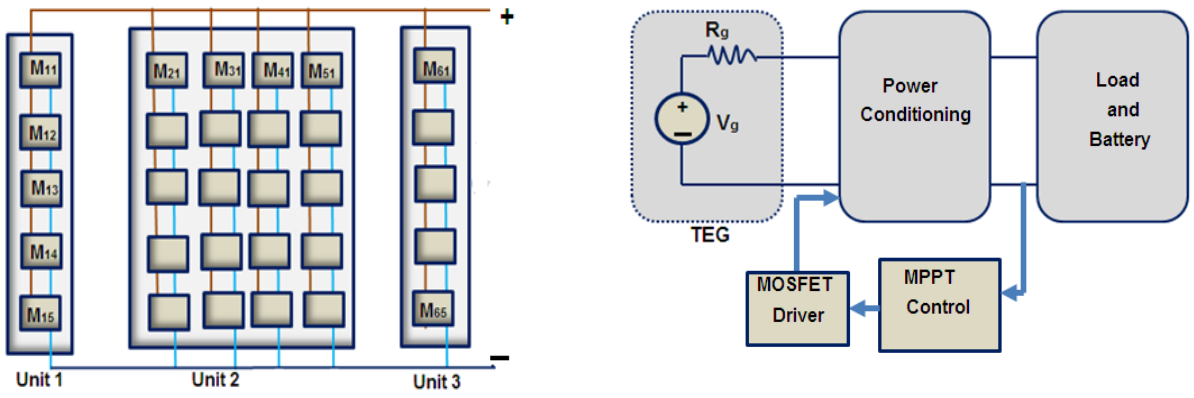

(a) Electrical connection of TEMs **(b)** TEG power conditioning.

Fig. 3: Connection diagram of the 30 modules by 3 units and equivalent circuit of TEG power conditioning.

3. Experimental setup

The experimental work was carried out in a 4 cylinder, 1.9698 L Volkswagen panel van diesel engine with common-rail direct injection system. The technical data for the vehicle and engine used are tabulated in **Table 1.**

Table 1: Vehicle and engine specifications

S/No.	Parameters	Values
1	**Vehicle**	Volkswagen panel Van/ 2.0 TDI
	Type	75kW SWB
	Weight (GVW)	2800 kg
2	**Engine**	4-stroke, 4cylinder
	Cylinder array	In line
	Swept volume	1968 (cm^3)
	Compression ratio	17:1
	Maximum power	75 kW @ 3000:3750rpm
	Maximum torque	250 Nm @ 2000:2500 rpm
	Bore	86 mm
	Stroke	92
3	**Fuel Consumption**	(litres/100km)
	Urban	7.9
	Extra urban	6.3
	Combined	7.5
4	**Transmission** (5-speed manual)	
	First gear ratio	4.2
	Second gear ratio	2.41
	Third gear ratio	1.36
	Fourth gear ratio	1
	Fifth gear ratio	0.78
	Differential ratio	4.84

3.1 Experimental of TEG module array configurations

In TE modules electrically connected systems, many TEM units are deployed in arrays with series and parallel bonds in order to achieve values greater than current and voltage. The method of correlation of TEGs is usually estimated by the desired voltage and current. The total output of voltage, current and power of TEG units array.

$$V_L = N_r V_o \quad I_L = N_c I_o \quad P_L = N_r N_c P_o \tag{12}$$

where N_r is the number of rows, N_c the number of columns and $N_r N_c$ the total number of modules in the array. A rectangular exhaust channel pipe with dimensions of (250× 310 × 75) mm^3 was fabricated in order to place a total of 30 customized TEMs with dimensions of (40 × 40 × 4) mm^3 on its two sides unit in a (1x5) and bottom side in a (4 × 5) arrangement. The specifications of the TEM power (TEG1B-12610-5.1) modules used are tabulated in **Table 2.**

Table 2: TE power (TEG1B-12610-5.1) modules specifications

S/No.	Parameters	Values
1	Size	40 mm · 40 mm
2	Open circuit voltage	7.2 V
3	Internal resistance	1.8Ω
4	Match load output-voltage	3.6 V
5	Match load output-current	2 A
6	Match load output-power	7.2 W
7	Heat flux density	≃9.2 W/cm^2
8	Heat flux across the module	≃148 W
9	Hot side temperature	300 ^{o}C
10	Cold side temperature	30 ^{o}C

The TEG device was mounted to exhaust channel pipe with the three especial aluminum sheets, and an aluminum heat sink with fins was mounted on the cold side of the TE modules, cold-side temperature at 40:48 ^{o}C, the TEMs cooling system is used the air tunnel system. Experimental connection of TE power generator of exhaust channel is shown in **Fig.4a, b.** The exhaust system of the Volkswagen vehicle tested is composed by the following parts: catalyst converter (CATC), diesel particulate filter (DPF), center muffler (CMUF), and rear muffler (RMUF), in order choose the position of TEG system. The temperature range was measured at all parts. The best position to install a TEG unit at CMUF, the temperature of CMUF acceptable with TE power (TEG1B-12610-5.1) modules specifications. **Fig. 4c** depicts the schematic of TEG kit position and the average temperature at the exhaust system parts. **Fig. 4c** depicts the TEG output power is obtained under the temperature difference and stored in load batteries from rectifier. The output of the TEG was connected to the engine electrical load and battery through a DC/DC converter requires setting approximately 14.5 voltages in order to charge the battery.

3.2. Measurements instrumentation

The main instruments used in the Volkswagen panel van diesel engines tests are:

- An eddy current chassis dynamometer was used for measuring the torque/speed engine output; the model is a SAXON TL-80 chassis dynamometer, it consists of a single roller (2WD) with a diameter of 168.54 cm. The dynamometer software used is able to program the driving conditions of the vehicle. Light duty engines are certified by the NEDC cycle, which is performed on a chassis dynamometer this paper uses dynamic programing to measure the emissions and the fuel consuming driving strategies **[44].** A wind simulation fan was placed in front of the vehicle to blow air over the car for cooling. Take a link of wind simulator to the airflow around TEG in cold-side, in order control of coolant the TEG cold

side by amount of air flow rate. The wind simulator controller operates to achieve blower speeds consistent with simulated vehicle velocity. **Fig. 4d** depicts the schematic of experiment vehicle installation.

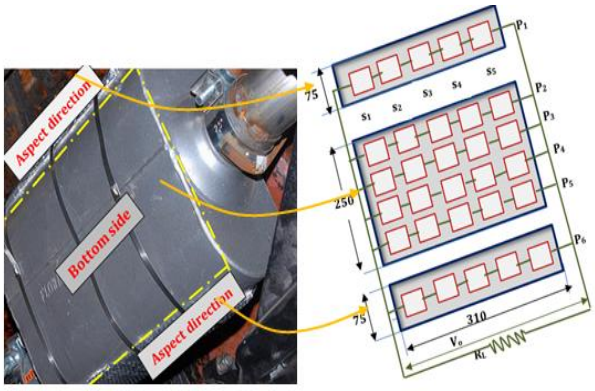

(a) Installation of TEMs

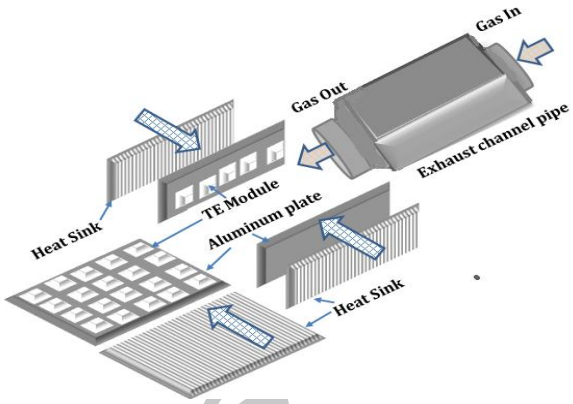

(b) Structure of TEG system

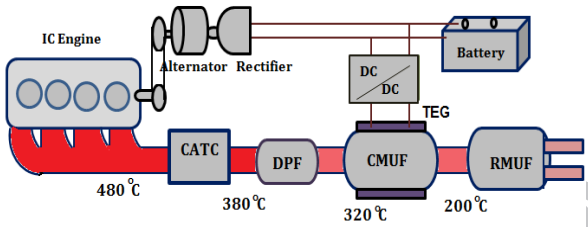

(c) TEG device select position and connecter to battery

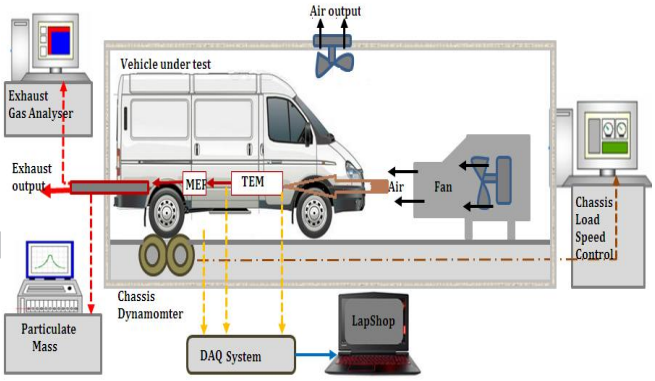

(d) Vehicle under testing

Fig. 4: Schematic diagram of the experimental installation.

- The exhaust gas flow rate was measured with raw exhaust gas flow-meter (VAV-EGF6); the principle operation is variable throat area venture-tube. The DFC was measured by vehicle control unit (CU) of the engine. The pressure drop across the TEG system was measured using a pressure transducer with differential pressure transmitter STD930.
- A HOMANS analyzer was measured the exhaust emissions of Total hydrocarbons THC (ppm), Carbon monoxide CO (vol.%), Carbon dioxide CO_2 (vol.%), and Nitrogen oxides NOx (ppm) concentrations. A smoke meter (LEX-04B) was measured the continuously the soot level of a sample of the exhaust flow from diesel engine, and the cumulative soot was calculated by multiplying the exhaust gas flow rate, mass soot concentration and integrating them **[44,45].**
- The electric voltage, current and power generated by the TEG modules was measured by PA2200 series power analyzer.

- The engine exhaust gas, TEG surface temperatures and ambient air temperature have been measured with K-type a thermocouple sensors. The measure signals recorded were passed to the DAQ. **[42].**

The range and accuracy of measured parameters are tabulated in **Table 3.**

Table 3: Range and accuracy of measured parameters

No.	Device type	Measured parameters	Measurement range	Accuracy	Units
1	Chassis dynamometer	Speed	0:10000	≤ 0.1%	rpm
2	Chassis dynamometer	Maximum power	0:180	≤ 0.12%	kW
3	Engine dynamometer	Maximum torque	0:300	≤ 0.1%	Nm
4	Thermocouple	Exhaust temperature	0:+1000	≤ 0.12%	°C
5	Power analyzer	Current	0:50	±0.2%	A
6	Power analyzer	Voltage	0:1000	±0.1%	V
7	Emission gas analyzers	NOx	0:5000	± 2	ppm
8	Emission gas analyzers	THC	0:3000	± 1	ppm
9	Emission gas analyzers	CO	0:20	± 0.002	Vo.%
10	Emission gas analyzers	CO_2	0:30	± 0.01	Vo.%
11	Raw exhaust gas flow-meter	Exhaust gas flow rate	0:5.5	±3%	m^3/min
12	Differential pressure transmitters	Differential pressure	0:100	±0.5%	psi

4. Results and discussions

4.1 The TEM characteristic with different engine speed

In this subsection presents the main experimental results of the analyzed system in terms of the output TGE power, TEG voltage, pressure drop, exhaust gases temperatures, TEM surfaces temperatures with vehicle engine different speeds, it has been that the vehicle engine operates (750, 1500, 2250, 3000, and 3750) rpm and engine no loaded.

4.1.1 Evaluation of TEM hot and cold surfaces temperature

The first part is focused on evaluate TEMs air cooling system of cold side, in order estimate the coolant air flow rate and measured the exhaust gases temperatures and TEM surfaces temperatures with vehicle engine different speeds. **Fig. 5** presents TEM surface temperatures with different engine speed at different flow rates on cold side (0%, 30%, 60% and 100% coolant air flow rate). The temperatures of the TEMs hot surface with 800s and constant engine speeds of 750, 1500, 3000 and 3750 rpm are respectively T_h= 90 °C, 135 °C, 225 °C and 270 °C. The time to reach maximum TEM hot surface temperature 800s, 730s, 200s and 160s in the vehicle engine speeds of 750, 1500, 3000 and 3750 rpm are respectively. It is evident the TEM hot surface temperatures increased quickly according to the engine speed increased, this result indicates that the TEM cold surface temperatures is slightly increased with time and engine speed. It is clearly seen that the coolant

air flow rate control on cold surface temperatures increased according to the engine full warm up. The control of coolant air flow rate has been simulated by fan speed and coolant air valve, in order to maintain T_C =40:48 °C.

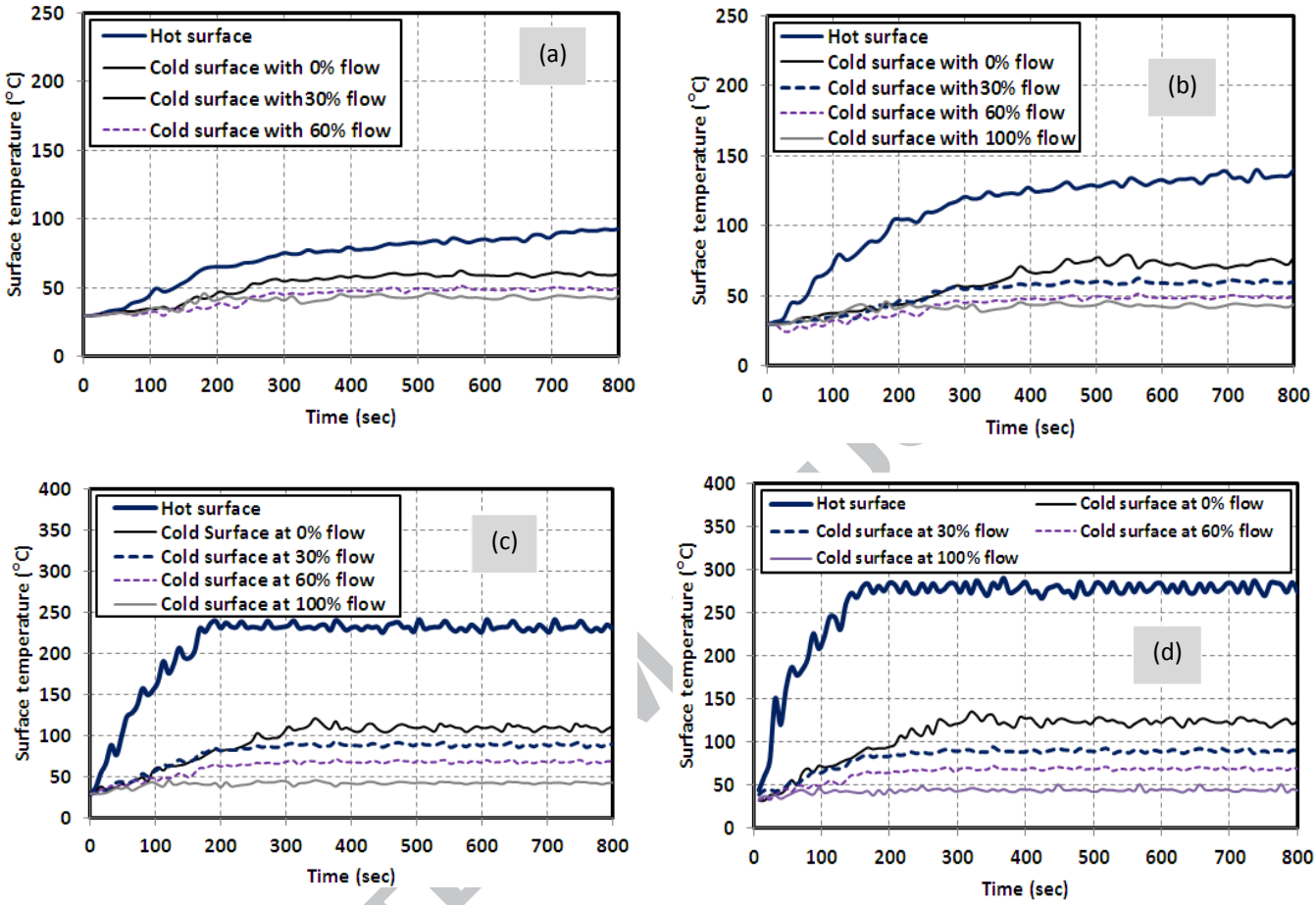

Fig.5: The TEM surface temperatures. (a)750 rpm, (b)1500rpm, (c) 3000rpm, and (d)3750 rpm.

The input and outlet temperatures of exhaust gas have been obtained and shown in **Fig. 6**a, the exhaust gas temperatures increase as a function of engine speed. It can be found that maximum temperatures of input and outlet are 340 °C and 300 °C respectively. **Fig. 6b** depicts the experimental hot and cold surfaces temperature of TEM module with different engine speed; this result indicates that the maximum TEM module temperature at high engine speed, the peak value of temperature is approximately 120 °C the cold surface side and 275 °C the hot surface. **Fig. 6c** illustrates the exhaust gas flow rate and pressure drop with different engine speed, the exhaust flow rate increase as a function of engine speed. The maximum exhaust flow rate is approximately 59 g/s at 3750 rpm. The variation of pressure drop about TEG with different engine speed, the

pressure drop is proportion with the engine speed, the pressure drop is 425 Pa at 750 rpm and it reaches 1095 Pa at speed 3750 rpm.

The TEG works between the exhaust line and the air flow to convert waste heat to electrical power. The experimental temperature of the hot side TEMs rises up to 275 °C, in these conditions the system works well for 800 sec (13.3 minut) .The maximum temperature of (TEG1B-12610-5.1) modules is 300 °C.

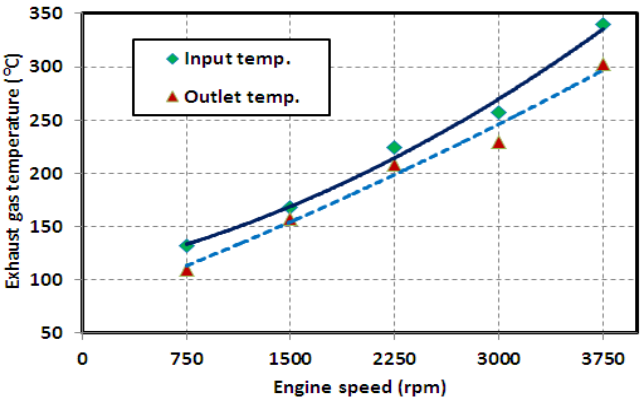

(a) The temperatures of exhaust gas

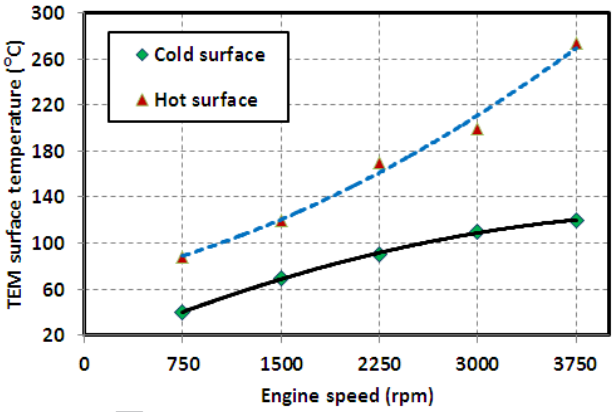

(b) TEMs surfaces temperature

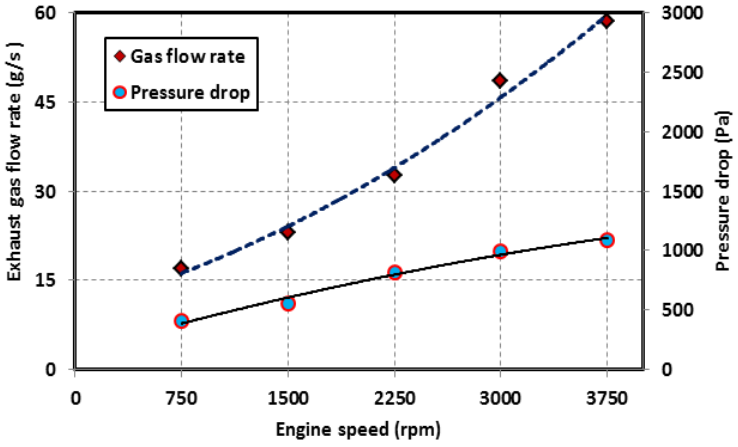

(c) Exhaust flow rate and pressure drop

Fig. 6: The measured temperatures, exhaust gas flow rate and exhaust pressure drop.

4.1.2 The TEG characteristic curves

The second part is focused of the theoretical and measured TEG output power, and evaluation of the maximum power point trend to be performed in controller. From **Fig. 6b** data can be estimated the difference of temperature across the couple $\Delta T = T_h - T_c$ with related engine speeds and shown in **table 4**.

Table 4: The difference of temperature across the couple at no load

Engine speed (rpm)	Cold surface temperature (^{o}C)	Hot surface temperature (^{o}C)	Temperature difference across the couple (^{o}C)	Pressure drop (Pa)
750	40.4	88	47.6	425
1500	70	120	50	550
2250	90.5	170	79.5	820
3000	110	200.7	90.7	990
3750	120	275	155	1095

Fig. 7a and **b** shows the TEG output power as versus of the current with different engine speed, it will be seen that the TEG output power increase with the vehicle engine speed. **Fig. 7c** and **d** shows the variation of TEG output power as versus of the applied load with different engine speed. It is observed that for maximum values of TEG power acting on applied load at constant engine speeds of 750, 1500, 2250, 3000 and3750 rpm are respectively P_L=55.4 W, 92.1 W, 129 W, 173.9 W and 214.7W in order to implement the MPPT technique, aligned with literature results **[14, 42].**

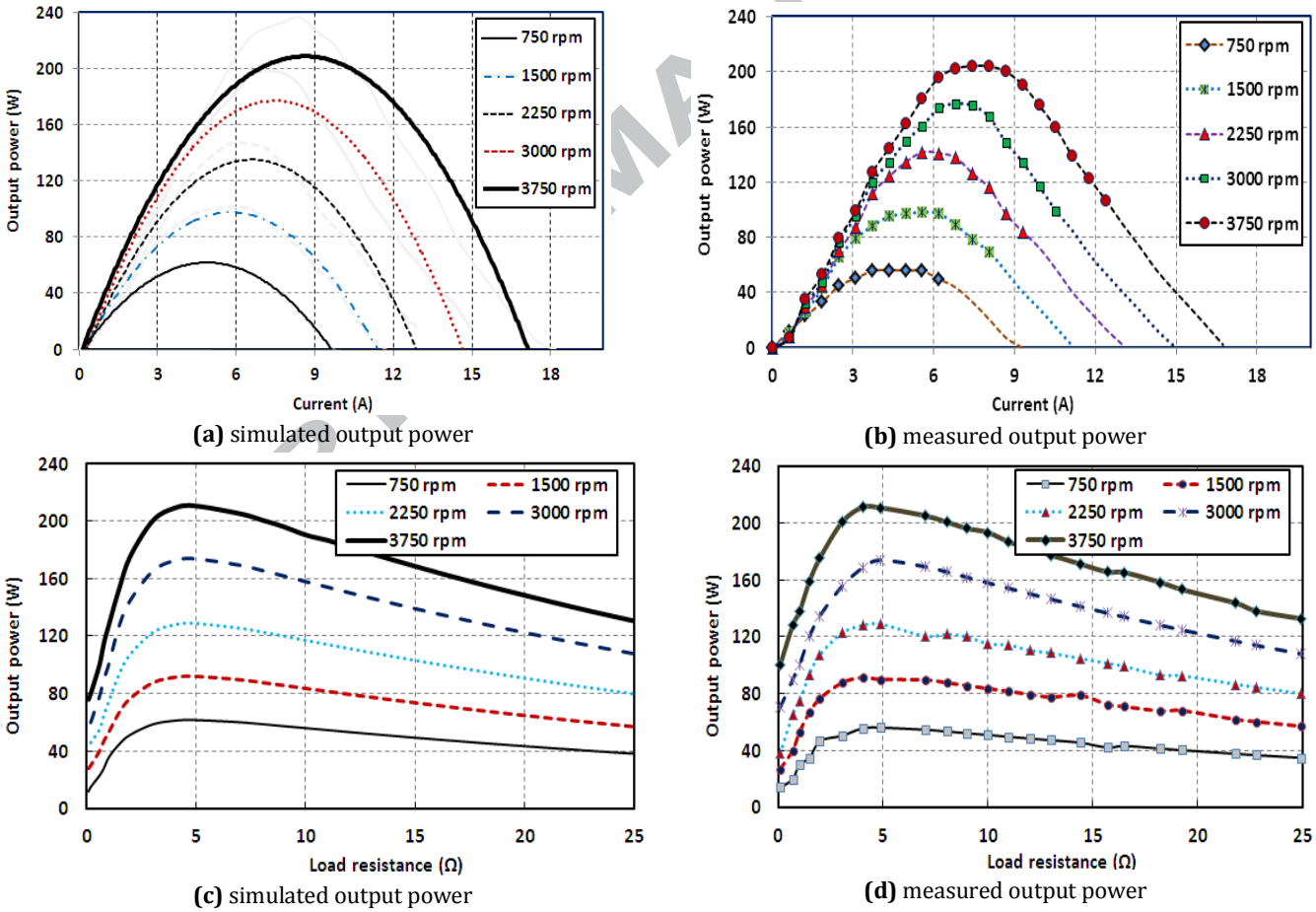

(a) simulated output power

(b) measured output power

(c) simulated output power

(d) measured output power

Fig. 7: The measured and simulated output of the TEG characteristic curves with different engine speed.

Fig. 8 depicts the error, average error and percentage of error between the simulated and measured output power. The average error of the output power is shown in **Fig. 8c**, it can be seen that average experimental result has an agreement with the average theoretical result within approximately 6-15 W error value for the engine speed lower than 3750 rpm. The percentage of error between the simulated and the measured power is shown in **Fig. 8d,** as it can be seen, the experimental result of power is in good agreement with the theoretical result within 5.16% error for the engine speed 1500 rpm.

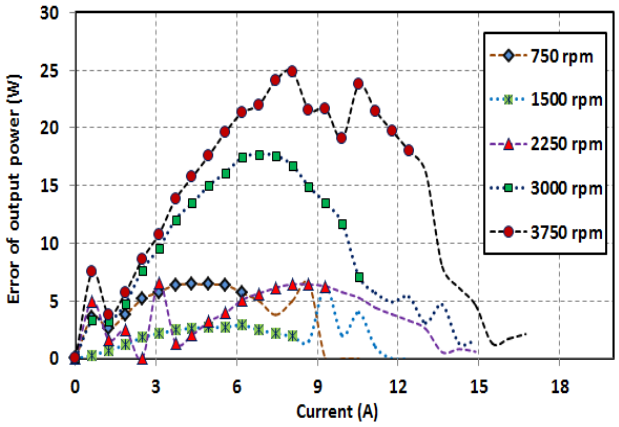

(a) Error output power with different current

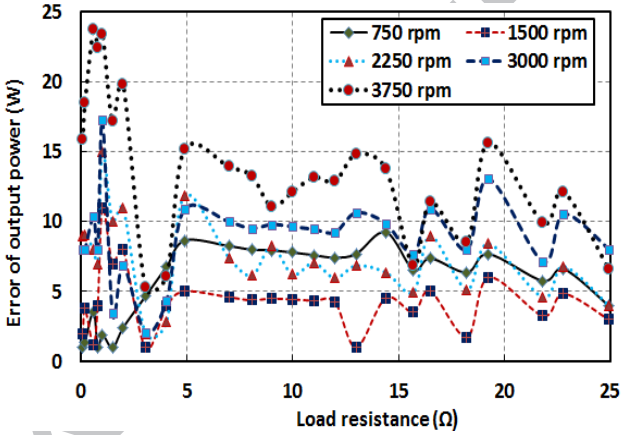

(b) Error output power with different resistance

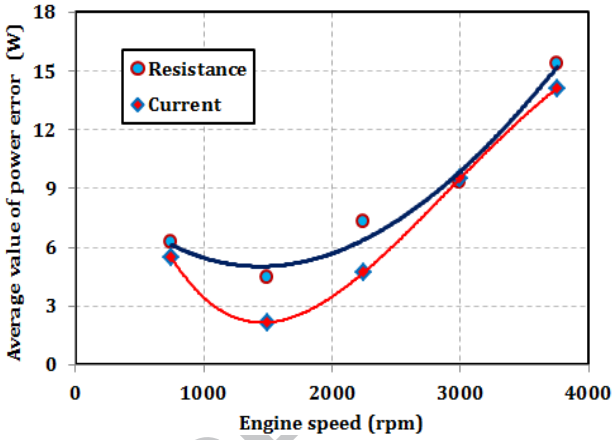

(c) Average error between the simulated and measured power

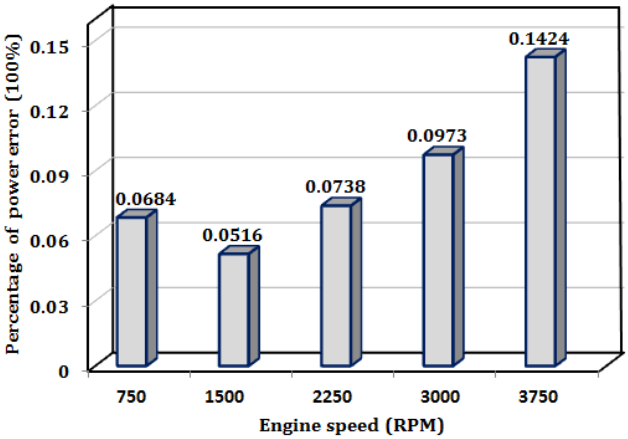

(c) Percentage of error between the simulated and measured power

Fig. 8: Error, average error and percentage of error between the simulated and measured output power

Fig. 9 shows the TEG output voltage, current and power as a function of time different engine speed. The TEG output power is proportional to the vehicle engine speed, the TEG output voltage, current and power an increase in the engine speed by improves the exhaust flow rate and heat recovery, the maximum TEG output power is approximately 214W at 3750 rpm, the maximum efficiency of TEG system is approximately 10.2% at 3750 rpm, aligned with literature results **[14,34].**

An electrical power conditioning and interface unit to match the power output of the thermoelectric modules to the vehicle battery **[46].** The TEG output power changes dynamically with the temperature of exhaust gas and change the engine speed, power conditioning between the TEG and the load battery is inevitable as shown in **Fig.3b.**

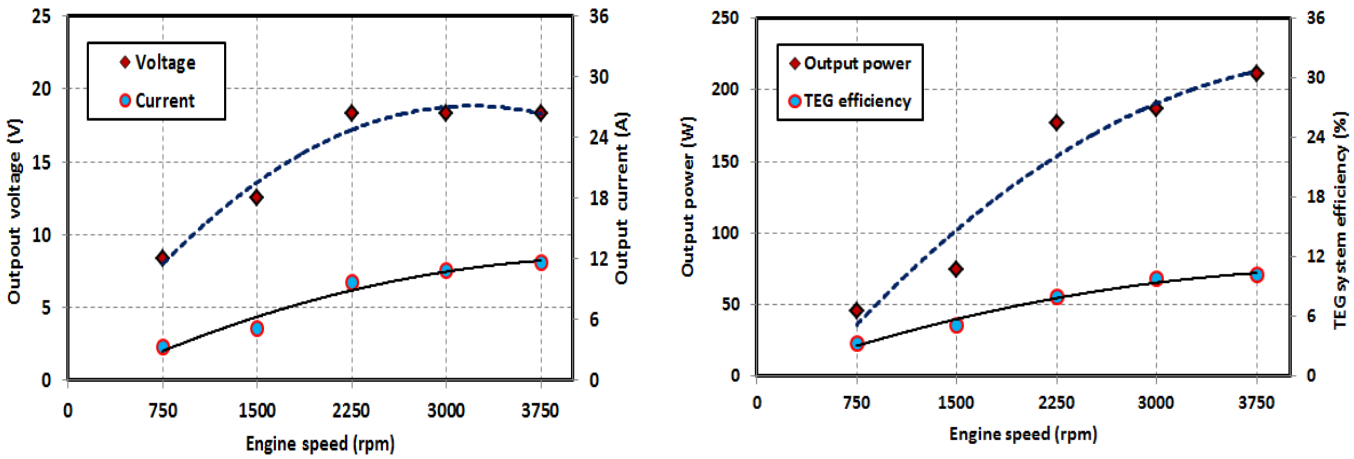

(a) TEG voltage and current

(b) TEG maximum power and efficiency

Fig. 9: TEG performance curves with different engine speeds.

4.2 The vehicle performance with TEG test under NEDC

The application for the TEG device is as a source of electrical power generation in motor vehicles in addition to the vehicle alternator **[40],** therefore the electrical load is covered by vehicle alternator when without activated TEG device, and its covered by TEG device and vehicle alternator at needed when activated TEG device, and each of them pours the electric output into the electric power grid of the vehicle. The test is applied with vehicle continuous electrical loads for range 200:220 W with and without activated the TEG device.

In this subsection presents the main experimental results of the analyzed system in terms of exhaust gases temperatures, TEM surfaces temperatures and available exhaust waste heat under the NEDC driving cycle. A comparative analysis of the exhaust mass flow rate, DFC, and exhaust emissions such as THC, CO, CO_2, NOx and smoke opacity emission has been measured under the engine operated with and without activated the TEG system.

4.2.1 Mass flow rate of exhaust gases and temperatures under the NEDC

Fig. 10a illustrates the exhaust gas temperatures at input and outlet of exhaust channel pipe. It can be found that in both maximum input and outlet exhaust temperatures, when the vehicle speed is high. **Fig. 10b** depicts the experimental surfaces temperature of TEM module under NEDC; this result shows that the

maximum TEM module temperature at high acceleration driver, the peak value of temperature is 102 °C the cold surface and 290 C° the hot surface.

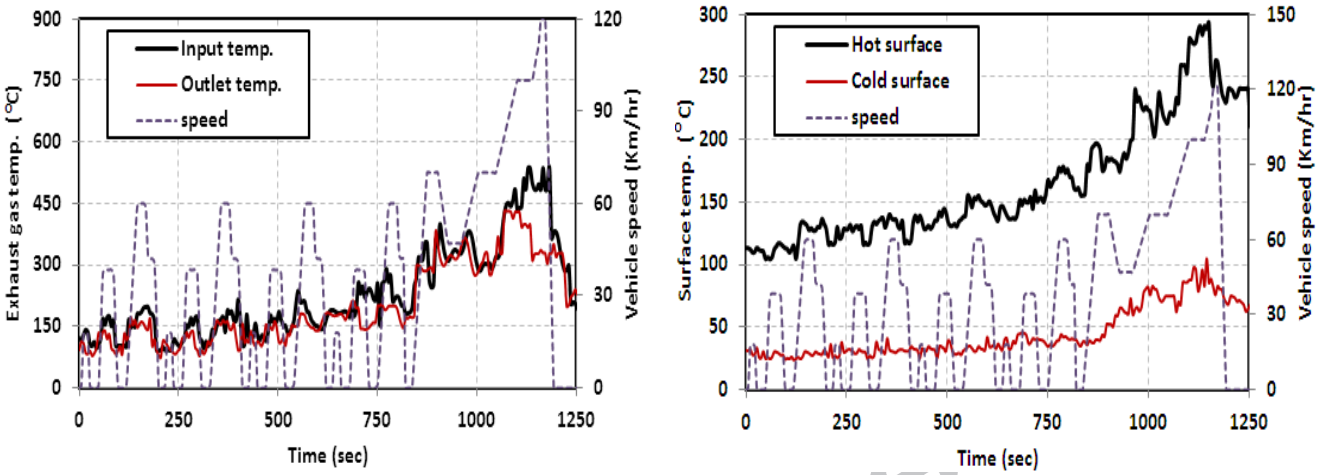

(a) Input and output temp. across TEG **(a)** Hot and cold surfaces temp. of TEG

Fig. 10: Exhaust gases temperatures and TEM surfaces temperature during the NEDC driving cycle.

Fig. 11 presents the mass flow rate of exhaust gases obtained with and without actuation TEG system during the NEDC driving cycle. The peak value of exhaust flow rate is approximately 68 g/s without actuation TEG and 50 g/s with actuation TEG system and the average value is 15.6 g/s without actuation TEG and 14.2 g/s with actuation TEG system, the reduction of average flow rate is 8.9% along time of NEDC, aligned with literature results **[34, 47].** It is calculated by $\bar{x} = (1/N)\sum_{n=1}^{N} x(n)$, where *N* is the number of samples and *x(n)* is mass flow rate of exhaust gases. The TEG output power is proportional to the engine rotation speed and the engine load, this is related to the amount of fuel and air mass flow rates. When the TEG system is actuated, the load is reduced on the alternator at a certain engine speed condition. In this case, the amount of fuel and air mass flow rates is decreased, and therefore the exhaust mass flow rate reduces.

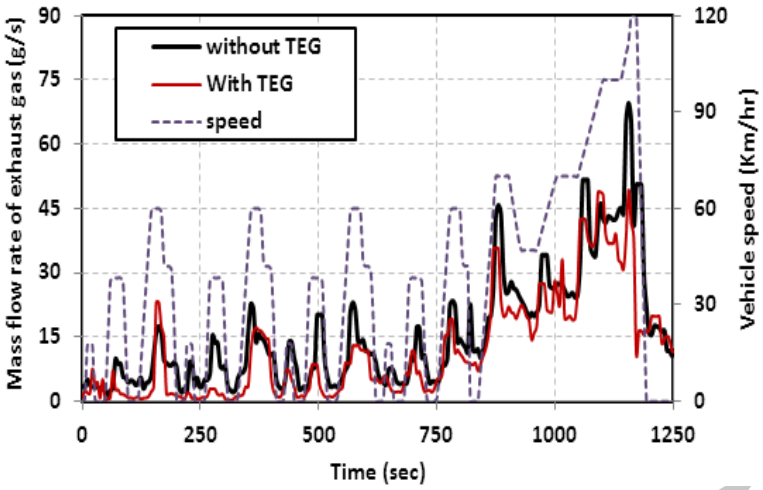

Fig. 11: The exhaust mass flow rate during the NEDC driving cycle.

4.2.2 TEG electric power and TEG system efficiency under the NEDC cycle

In this subsection presents the exhaust gas heat quantity (Q_{ex}) estimate for diesel engine was obtained from measure mass flow ($\dot{m}$) and temperatures (T_{ex}, T_{amb}) according to Eq.(1), the exhaust waste gas energy under the NEDC is shown in **Fig. 12.** The peak value of exhaust waste gas energy is approximately 11 kW under the NEDC, the average value of exhaust waste gas energy is 1.15kW for first part of cycle (urban cycle) and 5.48 kW for second part of cycle (extraurban cycle).

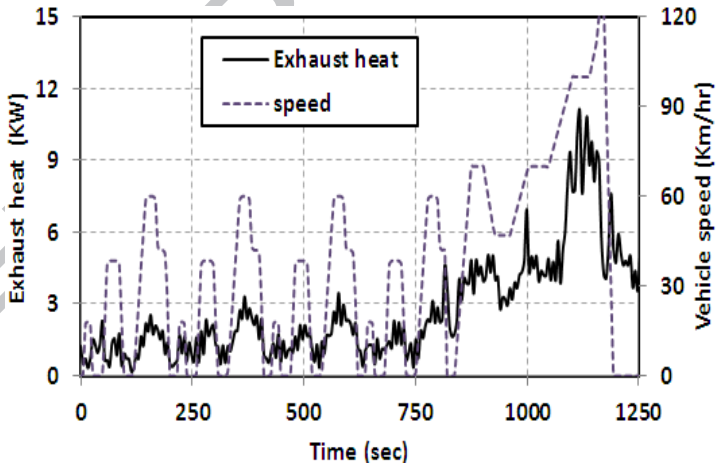

Fig. 12: Available exhaust waste heat during the NEDC driving cycle.

The electrical power generation curve under the NEDC is depicted in **Fig. 13a,** the peak value of the electrical power during along NEDC is approximately 392 W. The average value of electrical power is approximately 62 W for first part of cycle (urban cycle) and 212 W for second part of cycle (extraurban cycle). **Fig. 13b** presents the TEG system efficiency during the NEDC, the peak value of efficiency is approximately 22% under the NEDC. The average value of TEG system efficiency is approximately 4.63% under the NEDC. It is observed

that about 3.6–7% of the waste energy of exhaust gases can be transformed into useful energy in a recovery TEG system.

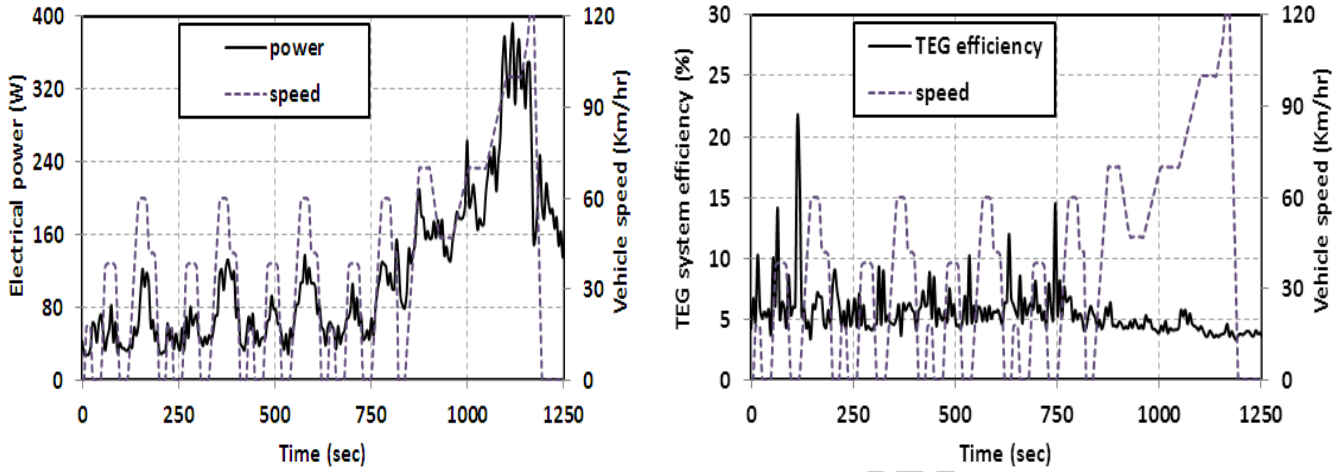

Fig. 13: Recovered TEG electric power and TEG system efficiency during the NEDC driving cycle.

4.2.3 Fuel consumption obtained with and without actuation TEG system

In this subsection presents the fuel consumption obtained with and without actuation TEG device, the vehicle test is applied continuous electrical loads at two cases, first case at TEG device not actuation (the alternator to supply an electrical load), second case at TEG device actuation (the TEG device to supply an electrical load)

Fig 14 shows the impact of TEG on instantaneous and cumulated DFC during the NEDC, It shows that most of the DFC in the last phase of the cycle at high acceleration driver (extraurban cycle) **[44]**, the maximum peak value of DFC is approximately 2.65 g/s without actuation TEG and 2.34 g/s with actuation TEG system, the reduction of average DFC is 2.3% along time of NEDC with actuation TEG system.

The cumulated DFC reduced between actuation TEG and without actuation TEG engine (baseline) are 1.46% at end of urban cycle and 3.13% at end of extraurban cycle. This indicates the effectiveness of the actuation TEG system for the DFC during NEDC. In the first case at TEG device not actuation, the DFC is higher for this case. Due to the direct mechanical connection between IC engine and alternator by a V-belt, consequently the alternator then takes the mechanical energy from the IC engine. But in the second case at TEG device actuation, the recovered electric power of the TEG device is used to supply the vehicle electrical load and battery charge (boost electrical circuit). Hence, the alternator is relieved. Consequently, the relief of the alternator from TEG also decreases the necessary drive power of the ICE and the DFC in particular.

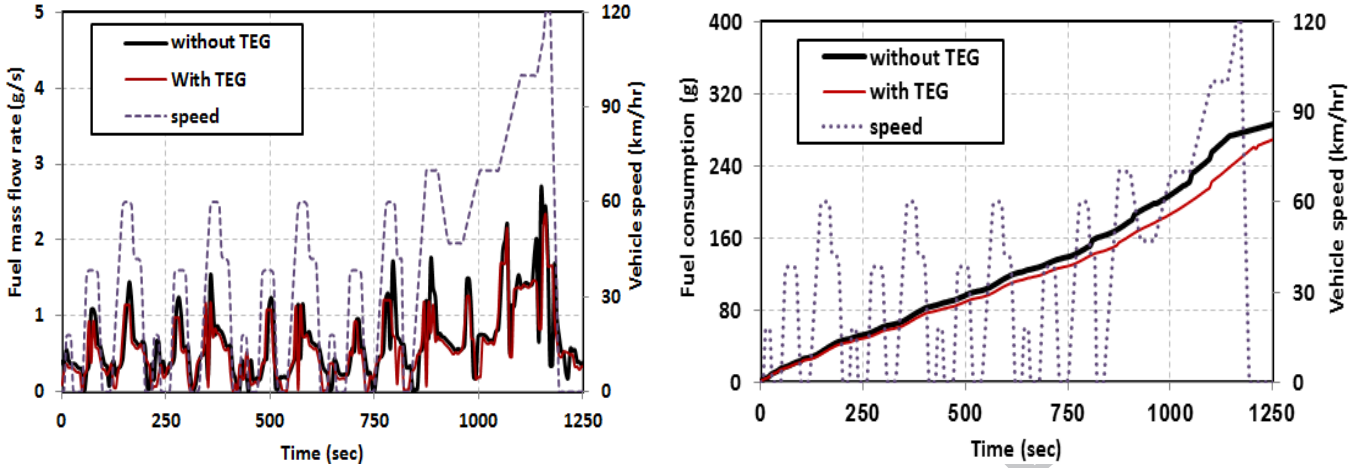

(a) Instantaneous fuel mass flow rate over the NEDC **(b)** Cumulated fuel consumption over the NEDC

Fig. 14: Fuel consumption obtained with and without actuation TEG during the NEDC driving cycle.

4.2. 4 Exhaust gas emissions obtained with and without actuation TEG system

Fig. 15 shows the experimental engine exhaust CO_2, and CO, THC, NOx emissions for the Volkswagen panel Van diesel operating over the NEDC. It is found that active TEG system produces lower level of exhaust gas emissions as compared to that produced by not actuation TEG system.

As it can be seen the maximum peak value of CO is approximately 0.72 vol. % for actuation n TEG system and 0.78 vol. % in case without actuation TEG system during NEDC, and it will be seen that maximum peak value of CO_2 17.6 vol. % for actuation TEG system and 14.7 vol. % in case without actuation TEG system during NEDC. The maximum peak values of THC and NOx emissions are approximately 205 ppm and 373 ppm respectively for not actuation TEG system and 194 ppm and 289 ppm of THC and NOx emissions respectively, with actuation TEG system. This indicates the effectiveness of the actuation TEG system for the vehicle exhaust during NEDC.

Fig. 16a illustrates the averages of CO_2 and CO diesel vehicle emissions under NEDC test, it is observed that a reduction of around 3.9% for CO_2 and 2.6% for CO, for the case of actuation TEG system to the case without actuation TEG system with urban cycle, and the reduction with extraurban cycle 6.2% for CO_2 and 4.3% for CO with actuation TEG system. The averages of THC and NOx diesel vehicle emissions under NEDC test are shown in **Fig. 16b.** Such level of decrease in average THC is around 4.4% and 3.7% of NOx emission, for the case of actuation TEG system to the case without actuation TEG system with urban cycle, and the reduction with extraurban cycle 6.1% for THC and 6.8% for NOx with actuation TEG system.

The combustion temperature is raised at critical values at high load so that the molecules of nitrogen and oxygen concentration combine under this condition NOx formation. The emission control systems of panel van diesel engine consist of the catalyst converter (CATC), diesel particulate filter (DPF), and Exhaust gas recirculation (EGR). The Exhaust gas recirculation (EGR) system is used to reduce the NOx emissions by lowering the flame temperatures in diesel engines.

The TEG cooling system is used the air tunnel system, the TEG system input and outlet temperatures of exhaust gas have been obtained and shown in **Fig. 6**a, as it can be seen in this figure the TEG system effect of exhaust temperatures. While using a TEG system that works to reduce the temperature of exhaust gases relatively, when the EGR system takes an exhaust gases into the combustion chamber, at this condition the EGR system is improved effectiveness. The utilization of both EGR and TEG strategies in internal combustion engines leads to numerous impacts affecting to an engine emission operation.

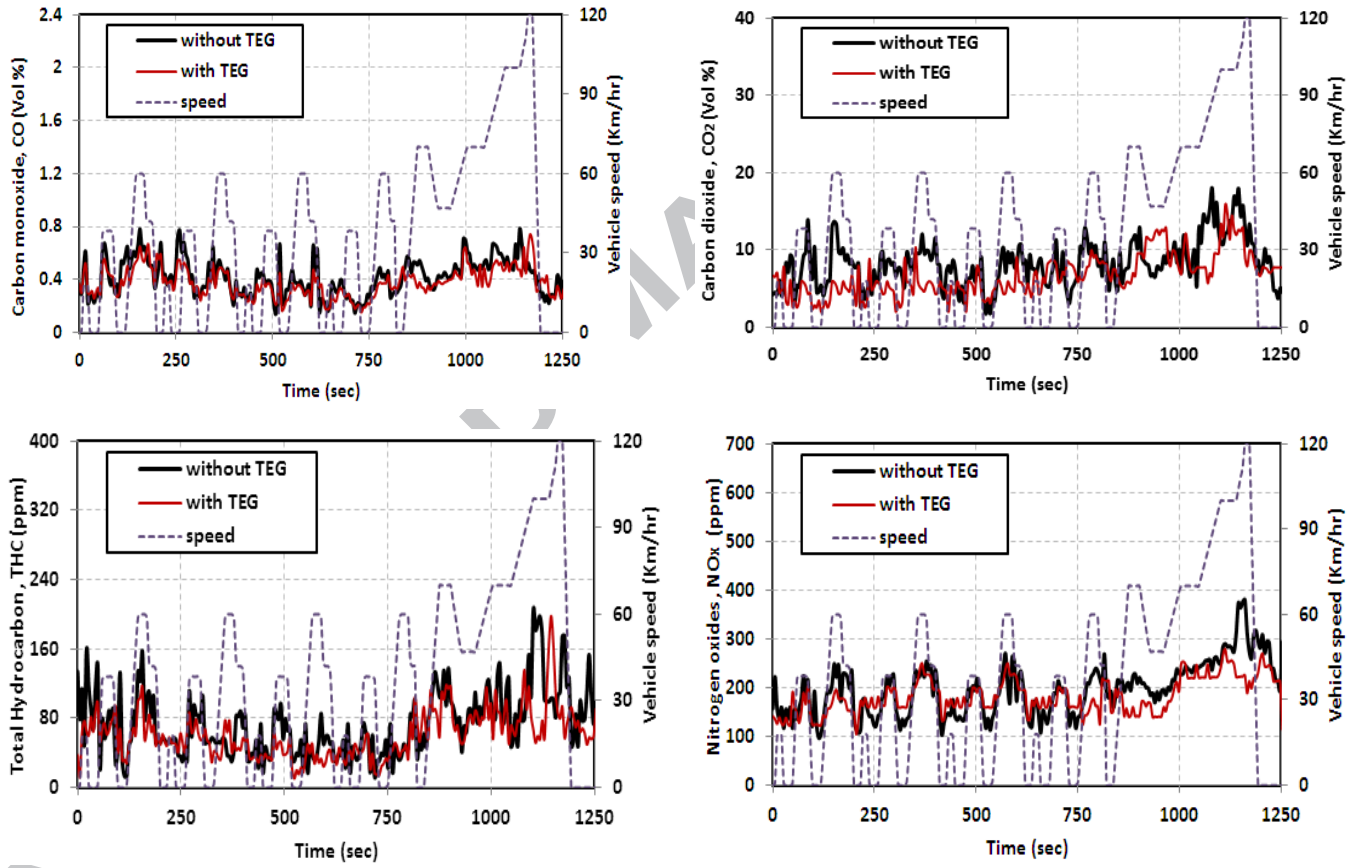

Fig. 15: CO, CO_2, THC and NOx emissions with and without actuation TEG during NEDC.

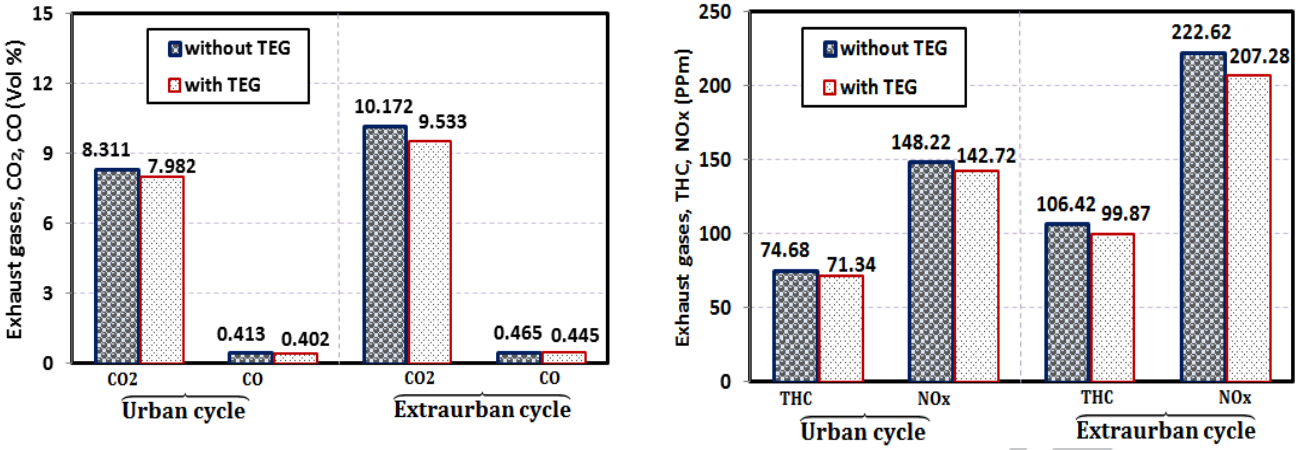

Fig.16: Average exhaust gas emissions with and without actuation TEG during NEDC.

Instantaneous smoke opacity emission measured with and without actuation TEG system is presented in **Fig. 17a**, this result marks that most quantity of the opacity in the last phase of the cycle, the instantaneous smoke opacity under the NEDC show the maximum peak value is approximately 32.6 % without actuation TEG and 29.7% for actuation TEG system. **Fig. 17b** depicts the accumulated mass of gas particles under the NEDC cycle. The reduction of particles with actuation the TEG was 5.17% at end of urban cycle and 6.46% at end of extraurban cycle.

The coalescing between engine alternator and TEG device in vehicle electric power grid is useful in DFC. Consequently; the CO, HC, CO_2 and smoke opacity emissions of the diesel engine can be reduced.

In overall analysis, this application of the TEG system in a diesel vehicle recovers output power. The electrical power of TEG system has been connected to the DC–DC boost converter and stored in vehicle battery (boost electrical circuit), this allows the alternator load to decrease, and the amount of fuel and air mass flow rates is decreased. Consequently the DFC and then the emissions are decreased slightly.

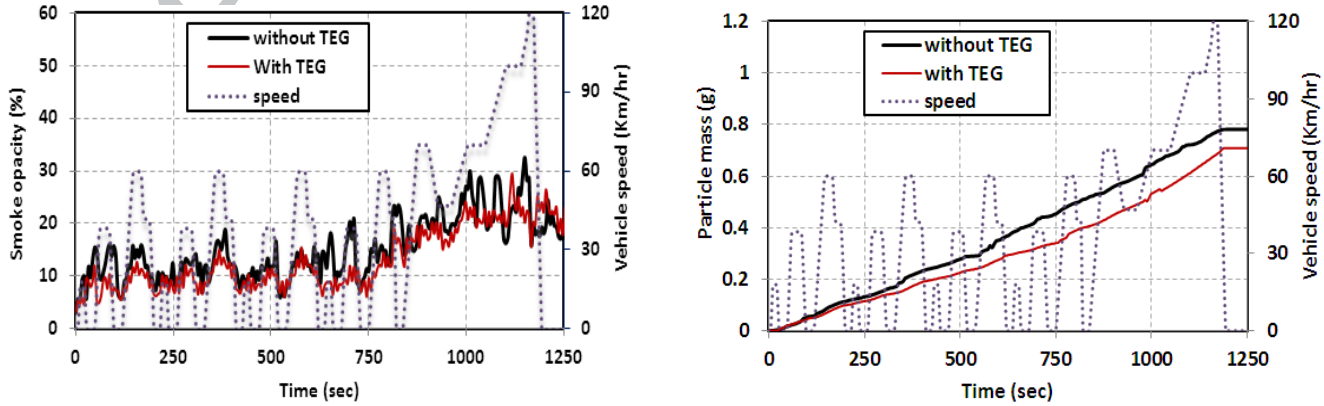

Fig. 17: Exhaust smoke opacity and accumulation of particle mass with and without actuation TEG during NEDC.

5. Conclusions

In this work, the development of thirty (TEG1B-12610-5.1) TEMs arrangement used in TEG system with evaluation of diesel engine DFC and emissions obtained under NEDC are presented. The main conclusions can be below from this study.

- The TEG system was mounted to the exhaust pipe of a light diesel vehicle in order to supply heat. The airflow around TEG has been simulated in the cold side to reject heat.
- The exhaust gas temperatures increase as a function of engine speed. It can be found that maximum temperatures of input and outlet are 340 °C and 300 °C at 3750 rpm respectively. The TEG output power is proportional to the vehicle engine speed; the maximum TEG output power is approximately 214W at 3750 rpm.
- The experimental result of output power is in good agreement with the theoretical result within 5.16% error at 1500 rpm.
- The peak value of the output power by TEG system during along NEDC is approximately 392 W and the average value of electrical power is approximately 62 W for first part of cycle (urban cycle) and 212 W for second part of cycle (extraurban cycle). The average value of TEG system efficiency is approximately 4.63% under the NEDC cycle.
- The DFC was evaluated based on the NEDC cycle, the results shown indicate that by actuation the TEG system, the DFC percentage has been reduced by1.46% at end of urban cycle and 3.13% at end of extraurban cycle. This indicates the effectiveness of the TEG system actuation for the DFC during NEDC cycle.
- The experimental results shown indicate that a reduction of exhaust gas emissions with actuation TEG system, and show the peak value is approximately 32.6 % without TEG system actuation and 29.7% for TEG system actuation of the smoke opacity under the NEDC.
- Finally, the coalescing between engine alternator and TEG device in vehicle electric power grid is useful in DFC. Consequently; the CO, HC, CO_2 and smoke opacity emissions of the diesel engine can be reduced.

References

[1] Shuhai Yu, Qing Du, Hai Diao, Gequn Shu, Kui Jiao (2015)"Effect of vehicle driving conditions on the performance of thermoelectric generator" Energy Conversion and Management 96 (2015) 363–376. http://dx.doi.org/10.1016/j.enconman.2015.03.002.

[2] Yang JH, Stabler FR. "Automotive applications of thermoelectric materials" Journal of Electronic Materials, 2009; 38(7),1245–51.

[3] Riffat SB, Ma X. "Thermoelectrics: a review of present and potential applications". Applied Thermal Engineering, 2003,23:913–935, https://doi.org/10.1016/S1359-4311(03)00012-7.

[5] Suter C, Jovanovic Z, Steinfeld A. (2012) "A 1 kWe thermo-electric stack for geothermal power generation - modeling and geometrical optimization". Applied energy, 2012, 99:379–385, https://doi.org/ 10.1016/j.apenergy.2012.05.033.

[6] Barros João (2013) "Performance measurement of thermoelectric generating plants with undesirable outputs and random parameters" International Journal of Electrical Power & Energy Systems, 2013, 46:228–233, https://doi.org/10.1016/j.ijepes.2012.10.019.

[7] Murat Demir and Ibrahim Dincer "Performance assessment of a thermoelectric generator applied to exhaust waste heat recovery" Applied Thermal Engineering, 120: 25, 2017, 694-707, https://doi.org/10.1016/j.applthermaleng. 2017.03.052.

[8] M. Kambe, (2004) "A Concept of 500 kWe Thermoelectric Power Conversion System to Make Use of Waste Heat of PWR Power Plant" Annual Research Report, Central Research Institute of Electric Power Industry, Japan, 2004.

[9] Min G, Rowe D. (2002) "Symbiotic application of thermoelectric conversion for fluid preheating/power generation. Energy Conversion and Management" 2002, 43:221–228, https://doi.org/10.1016/S0196-8904(01)00024-3.

[10] Liu X, Deng YD, Zhang K. (2014) "Experiments and simulations on heat exchangers in thermoelectric generator for automotive application" Applied Thermal Engineering, 2014;71:364–370, https://doi.org/10.1016/j.applthermaleng.2014.07.022.

[11] Liu X, Deng YD, Chen S. (2014) "A case study on compatibility of automotive exhaust thermoelectric generation system, catalytic converter and muffler" Case Stud Thermal Engineering ,2014; 2: 66–9, https://doi.org/10.1016/j.csite.2014.01.002.

[12]T.Y. Kim, A.A. Negash, G. Cho, (2016)"Waste heat recovery of a diesel engine using a thermoelectric generator equipped with customized thermoelectric modules", Energy Conversion and Management , 124 (2016) 280–6, https://doi.org/10.1016/j.enconman.2016.07.013.

[12]Weng Chien-Chou, Huang Mei-Jiau.(2013) "A simulation study of automotive waste heat recovery using a thermoelectric power generator" International Journal of Thermal Sciences, 2013,71:302–309, https://doi.org/10.1016/j.ijthermalsci.2013.04.008.

[13] Y. Y. Hsiao, W. C. Chang and S. L. Chen, (2010)"A Mathematic Model of Thermoelectric Module with Applications on Waste Heat Recovery from Automobile Engine," Energy, Vol. 35, No. 3, 2010, pp. 1447-1454. http://dx.doi.org/10.1016/j.energy.2009.11.030.

[14] Pandiyarajan V, Chinna Pandian M, Malan E, Velraj R, Seeniraj RV. (2011)"Experimental investigation on heat recovery from diesel engine exhaust using finned shell and tube heat exchanger and thermal storage system". Applied Energy, 2011;88:77–87. http://dx.doi.org/10.1016/j.apenergy.2010.07.023.

[15] O'Shaughnessy S, Deasy M, Kinsella C, Doyle J, Robinson A. (2013) " Small scale electricity generation from a portable biomass cookstove: prototype design and preliminary results". Applied Energy 2013;102:374–385. https://doi.org/10.1016/j.apenergy.2012.07.032.

[16] Champier D, Bedecarrats JP, Kousksou T, Rivaletto M, Strub F, Pignolet P. (2011) "Study of a TE (thermoelectric) generator incorporated in a multifunction wood stove". Energy 2011;36:1518–1526. https://doi.org/10.1016/j.energy.2011.01.012

[17] Nuwayhid R, Shihadeh A, Ghaddar N. (2005) "Development and testing of a domestic woodstove hermoelectric generator with natural convection cooling". Energy Converse Manage 2005;46:1631–43, https://doi.org/10.1016/j.enconman.2004.07.006.

[18] Viklund SB, Johansson MT. (2014) "Technologies for utilization of industrial excess heat: potentials for energy recovery and CO2 emission reduction". Energy Converse Manage 2014;77:369–379. https://doi.org/10.1016/j.enconman.2013.09.052.

[19] Ramadass YK, Chandrakasan AP. (2011) "A batteryless thermoelectric energy harvesting interface circuit with 35 mV startup voltage". IEEE J Solid-State Circuits 2011;46:333–41.

[20] Faraji A, Goldsmid HJ, Dixon C, Akbarzade A. (2015) "Exploring the prospects of thermoelectric power generation in conjunction with a water heating system". Energy 2015;90:1569–1574. https://doi.org/10.1016/j.energy.2015.06.121.

[21]M.F. Zhou, Y.L. He, Y.M. Chen, (2014) "A heat transfer numerical model for thermoelectric generator with cylindrical shell and straight fins under steady-state conditions" Applied Thermal Engineering. 68 (2014) 80-91, https://doi.org/10.1016/j.applthermaleng.2014.04.018.

[22]Gaowei Liang, Jiemin Zhou , Xuezhang Huang (2011) "Analytical model of parallel thermoelectric generator" Applied Energy 88 (2011) 5193–5199, https://doi:10.1016/j.apenergy.2011.07.041

[23] Zhang HJ, Chen H, et al. (2001)"Research on the generating performance of series-parallel connection and reappearance of a semiconductor thermoelectric module" Acta Energiae Solaris Sinica 2001;22(4):394–7

[24] Eakburanawat J, Boonyaroonate I. (2006) "Development of a thermoelectric battery charger with microcontroller-based maximum power point tracking technique" Applied Energy 2006;83:687–704, https://doi.org/10.1016/j.apenergy.2005.06.004, https://doi.org/10.1016/j.apenergy.2005.06.004.

[25] Kuo, Y. C., T. J. Liang, and J. F. Chen, (2001)"Novel Maximum- Power - Point Tracking Controller for Photovoltaic Energy Conversion System" *IEEE Transactions on Industrial Electronics*, Vol. 48, No. 3, 594-601, 2001.

[26] Kim, R. Y., and J. S. Lai, (2008)"Aggregated Modeling and Control of a Boost - Buck Cascade Converter for Maximum Power Point Tracking of a Thermoelectric Generator, *Proceedings of IEEE Applied Power Electronics Conference and Exposition*, 1754 -1760, 2008.

[27] Chuang Yu , K.T. Chau (2009)"Thermoelectric automotive waste heat energy recovery using maximum power point tracking" Energy Conversion and Management, 50 (2009) 1506–1512. https://doi.org/10.1016/j.enconman.2009.02.015.

[28] Vazquez J, Sanz-Bobi M, Palacios R, et al. (2002) "State of the art of thermoelectric generators based on heat recovered from the exhaust gases of automobiles". In: Proceedings of the seventh European workshop on thermoelectrics; 2002.

[29] Sumeet Kumar, Stephen D. Heister, Xianfan Xu, James R. Salvador, and Gregory P. Meisner,(2013) "Thermoelectric Generators for Automotive Waste Heat Recovery Systems Part I: Numerical Modeling and Baseline Model Analysis," Journal of Electronic Materials, Volume 42, Issue 4, 665-674, 2013.

[30]] Mori, M., Yamagami, T., Oda, N., Hattori, M. et al., "Current Possibilities of Thermoelectric Technology Relative to Fuel Economy," SAE Technical Paper 2009-01-0170, 2009, https://doi.org/10.4271/2009-01-0170.

[31] Karri MA, Thacher EF, Helenbrook BT. (2011) "Exhaust energy conversion by thermoelectric generator: two case studies" Energy Conversion and Management ,2011;52 (3):1596–611, https://doi.org/10.1016/j.enconman.2010.10.013.

[32] Nicholas K., Yanliang Z. "Design and optimization of automotive thermoelectric generators for maximum fuel efficiency improvement" Energy Conversion and Management 121 (2016) 224–231

[33] Boretti A. Transient operation of internal combustion engines with Rankine waste heat recovery systems. Applied Thermal Engineering, 2012; 48:18–23. http://dx.doi. org/10.1016/j.applthermaleng. 2012.04.043.

[34] Andrés F., Reyes García, John R., Octavio A. (2016)"Potential for exhaust gas energy recovery in a diesel passenger car under European driving cycle", Applied Energy. 174 (2016) 201–212, https://doi.org/10.1016/j.apenergy.2016.04.092.

[35] Liebl J, Neugebauer S, Eder A, Linde M, Mazar B, Stütz W. The thermoelectric generator from BMW is making use of waste heat. MTZ Worldw 2009;70:4–11.

[36] Ivan A, Andrea C, Cesare Pa, Vincenzo R, Matteo C" Modeling Analysis of Waste Heat Recovery via Thermo-Electric Generator and Electric Turbo-Compound for CO2 Reduction in Automotive SI Engines" Energy Procedia 82 (2015) 81 – 88, ATI 2015, doi: 10.1016/j.egypro.2015.11.886.

[37]Arsie, I., Cricchio, A., Marano, V., Pianese, C. et al., (2014)"Modeling Analysis of Waste Heat Recovery via Thermo Electric Generators for Fuel Economy Improvement and CO2 Reduction in Small Diesel Engines," SAE Int. J. Passeng. Cars –Electron. Electr. Syst. 7(1):2014, https://doi.org/10.4271/2014-01-0663.

[38]Liu X, Deng YD, Li Z, Su CQ. (2015) "Performance analysis of a waste heat recovery thermoelectric generation system for automotive application" Energy Convers Manage 2015;90:121–7.

[39]Pratiksha P., Pooja A., Pragati P., S. G. Tikhe (2015) "Automotive Waste Heat Harvesting for Electricity Generation using Thermoelectric Generator A Review" International Research Journal of Engineering and Technology, 5 2018 (2),477-481.

[40] Jihad Haidar , JamilGhojel (2001) " Waste heat recovery from the exhaust of low-power diesel engine using thermoelectric generators" 20th International Conference on Thermoelectrics, 2001, (Cat. No.01TH8589) IEEE, 413-417.

[41]Jensak E., Itsda B. (2006) "charger with microcontroller-based maximum power point tracking technique" Applied Energy, 83 (2006) 687–704.

[42]R. Palacios, A. Arenas, R.R. Pecharromán, F.L. Pagola (2009) "Analytical procedure to obtain internal parameters from performance curves of commercial thermoelectric modules" Applied Thermal Engineering, 29 (2009) 3501–3505, https://doi.org/10.1016/j.applthermaleng.2009.06.003.

[43]Andrea Montecucco and Andrew R. Knox (2015) "Maximum Power Point Tracking Converter Based on the Open-Circuit Voltage Method for Thermoelectric Generators, IEEE Transactions on Power Electronics 2015, 30, Issue:(2), 828 – 839, https://doi.org/ 10.1109/TPEL.2014.2313294.

[44] Eid S. Mohamed (2016)"Development and analysis of a variable position thermostat for smart cooling system of a light duty diesel vehicles and engine emissions assessment during NEDC" Applied Thermal Engineering ,99 (2016) 358–372, https://doi.org/10.1016/j.applthermaleng.2015.12.099.

[45] C. Arcoumanis, A. Megaritis, (1992) "Real-time measurement of particulate emissions in a turbocharged DI Diesel engine", SAE paper 922390, 1992.

[46] Eleni Avaritsioti (2016) "Thermoelectric Generator: An Electronic Device for the Reduction of CO_2 Emissions in Commercial Vehicles, Int. Journal of Energy and Environment 10, 2016, 219-224.

[47] İlker Temizer , Cumali İlkılıç (2016)"The performance and analysis of the thermoelectric generator system used in diesel engines, Renewable and Sustainable Energy Reviews,63 (2016)141–151, https://doi.org/10.1016/j.rser.2016.04.068.

Appendix

Nomenclatures

C_p	The heat capacity of the exhaust gas
K	Thermal conductivity of the material
K_c	The total cold-side thermal conductivity
K_h	The total hot-side thermal conductivity
I	Output current
N	The number of samples
N_c	The number of columns
N_r	The number of rows
P	The generated power
Q	Heat input
$\dot{m}$	The gas flow rate
Q_h	Heat source
Q_c	Rate of heat removal
R_C	The internal electrical resistance
R_L	The load resistance
T	The average temperature between hot and cold surfaces of the TEG
T_{amb}	The ambient temperature
T_C	Cold-side temperature
T_{ex}	The exhaust gas temperature
T_h	Hot-side temperature

V_O	Output voltage
V_S	The voltage at the terminals for series array's
V_P	The voltage at the terminals for parallel array's
$x(n)$	The variable parameters
ZT	The figure of merit

Abbreviations

ADC	Analog-to-digital converter
CATC	Catalyst converter
CO	Carbon monoxide
CO_2	Carbon dioxide
CMUF	Center muffler
DAQ	Data acquisition system
DFC	Diesel fuel consumption
DPF	Diesel particulate filter
EFC	Engine fuel consumption
MOSFET	The power metal–oxide–semiconductor field-effect transistor
MPPT	Maximum power point tracking
NEDC	New European drive cycle
NOx	Nitrogen oxides
RMUF	Rear muffler
PWM	pulse-width-modulated
TEG	Thermoelectric generation
TEMs	Thermoelectric modules
THC	Total hydrocarbons
2WD	2 wheel derive

Greek symbols

α	The Seebeck coefficient
δ	Electrical conductivity
ΔT	Temperature difference
η_{th}	Efficiency of thermoelectric element

Highlights

- A new procedure for the TEMs arrangement was proposed.
- An experimental work was carried out to study the performance of TEG system with different engine speed and during NEDC.
- The effect of TEG system on exhaust mass flow rate, DFC and exhaust emissions is quantitatively investigated.
- The average value of TEG system efficiency is approximately 4.63%.
- The average of DFC percentage has been decreased slightly by 2.3% with actuation TEG system over NEDC.